Creep Deformation and Rupture of Polycrystalline Alumina

D. KRAJCINOVIC, L. WEI and A. STOJIMIROVIC
CEMM Department, University of Illinois at Chicago, Chicago, IL 60680, USA

ABSTRACT

The paper presents a simple micromechanical model for the creep deformation of polycrystalline vitreous alumina. The inelastic strain is attributed to the grain boundary sliding and intergranular microcracks.

KEYWORDS

Micromechanics, creep deformation, polycrystalline ceramics.

INTRODUCTION

As a popular refractory material ceramics are often exposed to relatively high stress levels and very high temperatures for prolonged periods of time. Consequently, the components manufactured from ceramics are especially sensitive to creep deformation and creep rupture.

The macroscopic (phenomenological) signature of the process known as creep is a gradual increase in deformation at constant stress levels. Thus, the elastic stretching of the crystalline lattice is responsible only for a fraction of the total deformation. A variety of distinctly different mechanisms of the irreversible rearrangements of the mesostructure of the solid such as: grain boundary sliding, grain boundary and bulk diffusion, nucleation and growth of voids and grain size cracks, etc. are other significant contributors to the deformation process. The relative significance of a particular mechanism varies in dependence of the crystalline structure (chemical composition, grain size, presence of the second phase, precipitates, etc.) and the temperature and stress levels.

BASIC ENERGY DISSIPATION MECHANISM

The present study will focus on the Al_2O_3 alumina with a glassy inter-granular phase exposed to a homologous temperature of 0.5. The specimen will be subjected to uniaxial tension of 50 MN/m². For convenience only the case of plane strain will be considered. The average grain size is taken to be 50μm, while the thickness of the grain boundary phase is only 10nm. Under these conditions the final failure occurs as a result of the intergranular creep fracture (Frost and Ashby 1982).

In the considered case the alumina grains will remain perfectly elastic and, therefore, responsible primarily for the instantaneous, elastic response of the specimen. The time- dependent part of the deformation is traceable initially to the grain boundary sliding (viscous flow of the glassy phase). As the deformation increases the stress concentrations attendant to the geometrical nonconformity (keying of grains) and glassy phase pile-ups at triple joints may exceed the rupture strength of the atomic bonds. The nucleating and growing cracks will provide an additional source of the time-dependent inelastic strain. As those initially grain size cracks grow they eventually become responsible for the ultimate failure. For simplicity the present study will concentrate on the more frequent case when the grain size cracks are only intergranular. In the considered case of uniaxial tension the ultimate failure occurs as a result of the runaway (unstable) propagation of the critically oriented and situated crack kinking on the sequent grain boundaries. Even at failure the microcrack density levels are moderate.

The strategy common to most micromechanical modelling is to isolate the basic (dominant) energy dissipating mechanism, describe its kinetics and homogenize the derived equations into relations (1) mapping macrostresses on macrostrains. In the case considered in this paper the energy is dissipated on the formation and growth of the crack like defects within the glassy GB phase. It is also assumed that the ceramic material contains microcracks at the TJs which are traceable to the manufacturing processes. They are assumed to be small in comparison with the length of the GB. The geometry of the TJ is depicted in Fig.1.

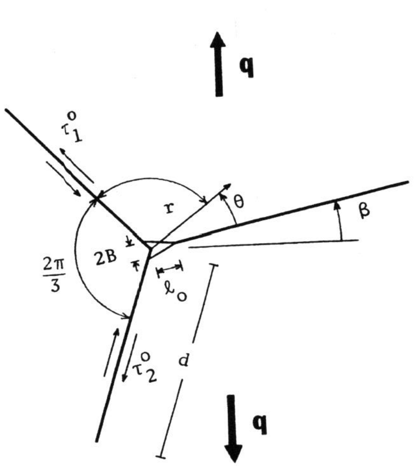

Fig.1 The geometry of triple grain junction

The determination of the inelastic stresses as a function of time (at constant magnitude of the externally applied traction q) requires consideration of the microcrack propagation along the GBs. The grain boundary sliding driven by the shear stresses along the slanted GBs increases the wedging effect and tends to increase the stress concentration at the far end and, consequently, the crack length itself. In contrast, the diffusion tends to relax the stress concentrations (Evans, et al. 1980, Raj 1975, Riedel 1987, etc.). Depending on the rate at which the two processes (GB sliding and diffusion) develop a crack at the TJ may or may not grow.

Assuming that a TJ crack will grow, after the stress intensity factor exceeds some threshold value, a crack will generally get arrested as it reaches the far end TJ. At this point further increase in the GB sliding caused wedging will be needed to kink the crack on the sequent GB and recommence growth.

The major problem in pursuing this strategy is related to a believable estimate of the stress intensity factor at the tip of the wedge TJ crack. The actual problem, due to the crystalline anisotropy (Tvergaard and Hutchinson 1987) and the presence of the two inclined GBs is not amenable to a closed form, analytical solution. For the present purposes it appears reasonable to start with a rather rough estimate assuming the surrounding material to be isotropic. Moreover, the influence of the sliding GBs will be assessed using finite element (FE) computations. Their effect will, subsequently, be introduced as a correction of a simple formula available in the literature for a wedged crack under the influence of far field tensile stresses. The stress concentration at the far end of the crack may in that case be written (Das, Marcinkowski 1972) as a sum of two terms

$$K = C \frac{EB}{4(1-\nu^2)} (\pi a)^{-\frac{1}{2}} + \sigma_n^o (\pi a)^{\frac{1}{2}} \qquad (1)$$

representing the contributions of wedging (2B being the crack opening at the TJ) and the far field tensile stresses ($\sigma_n^o = q \cos^2 \beta$) being the stress normal to the GB along which the crack propagates - assumed to be constant). Also, $2a = \ell_o$ is the length of the slit. The coefficient C is introduced to account for the boundary conditions along the sliding GB. Using enhanced elements the FE computations indicate that C=1 for $2a < \ell/3$, while for $2a=\ell$, C = 0.424. The residual stresses resulting from the thermal amisotropy (Evans, 1984) will be neglected hereafter.

The wedge opening 2B is, obviously, directly related to the amount of the shear deformation over the inclined GBs. The viscous glide of the glassy GB phase is, in general, resisted by the viscosity of the phase, irregularities of the GB, particles along the GB and keying of the grains (see Raj 1975, Riedel, 1987). Even though the keying action may have in the case of thin GB layers a rather significant effect on the sliding (see Tvergaard 1984), for simplicity, it will be assumed than for a thicker GB phase it can be neglected. Hence, the displacement discontinuity along the sliding GB can be directly related to the shear stress associated with the externally applied tensile tractions

$$\dot{u}(t) = \tau^o / \eta \qquad (2)$$

where

$$\eta = \frac{kTp^4}{8\Omega(\delta D_b + pD_v/5)\lambda^2} \tag{3}$$

is the friction coefficient depending (see Riedel 1987) on the size and distance between particles p and λ, GB and volume diffusion coefficients δD_b and D_v, atomic volume Ω and temperature T.

From geometry in view of (2) the growth of the wedge with time is

$$B(t) = \frac{\sqrt{3}}{4\eta}(\overset{o}{\tau}_1 + \overset{o}{\tau}_2) = \frac{3}{9\eta} qt \cos 2\beta \tag{4}$$

As the wedge opening $B(q,\beta,t)$ increases with time so does the stress intensity factor (1). The maximum stress at the far end crack tip can be written from (1) and (4) (integrated with respect to time) as

$$\sigma_y(t) = k(t)\ x^{-\frac{1}{2}} \tag{5}$$

where

$$k(t) = \dot{k}t + k_o = C\,\frac{3\ Eq \cos 2\beta}{16\pi\ \eta\ \sqrt{2a}}\ t + \frac{1}{2}\ q\ \sqrt{2a}\ \cos^2\beta \tag{6}$$

This stress is simultaneously relaxed by the process of diffusion (see Evans, et al. 1980). Even though the diffusion is, in general, a rather slow process the stress paths are in the case of stress concentrations exceedingly short. Thus, substantial stress relaxations may occur within very short time intervals. Noting that the stress is a linear function of time it is possible to use the results from (Evans, et al. 1980) and write

$$\sigma_y(t) = 0.89\ \dot{k}t\ (\alpha t)^{-1/6} + 0.74\ k_o\ (\alpha t)^{-1/6} \tag{7}$$

where

$$\alpha = \frac{G\delta D_b\Omega}{2(1-\nu)\kappa T} \tag{8}$$

It is noted that the stress is actually somewhat larger slightly ahead of the crack. However, for the value of αt considered in this paper this distance is very small. Hence, it will be assumed that the maximum stress is at the far end tip of the crack and that (7) represents a reasonably good estimate of the stresses which may cause the crack growth.

The crack will commence growing from its initial length $2a = l_0$ when the maximum stress near the crack tip exceeds the ideal bond strength of the material (Riedel 1987)

$$\sigma_y(0,t) = \sigma_{id} = m\left(\frac{E\gamma_s}{b_o}\right)^{\frac{1}{2}} \tag{9}$$

Thus, for given q and

$$F(\beta,t) = \frac{k(\beta,t)}{\sqrt{b_o}} - m\left(\frac{E\gamma_s}{b_o}\right)^{\frac{1}{2}} = 0 \tag{10}$$

represents a relation defining the crack length as a function of time. In (10) m = 0.52 to 0.86 is a dimensionless number, γ_s the surface energy and b_o the interatomic distance.

The condition (10) leads to a quadratic equation in the square root of the crack length a

$$\cos^2\beta\ (\sqrt{2a})^2\ -2.70(\alpha t)^{1/6}\ \frac{\sigma_{id}}{q}\ (\sqrt{2a})\ + 0.14\ C\ \frac{E}{\alpha\eta}(\alpha t)\cos 2\beta = 0 \tag{11}$$

from which it becomes possible to determine $a = a(\beta,t)$ for a given case of loading and given material parameters. For typical values of material parameters (see Riedel 1987, p. 9) the discriminant of the quadratic equation (11) is always positive even for crack lengths measured in millimeters. Consequently, cracks grow monotonically with time from their initial length until they reach the far end TJ of the GB.

When the intergranular crack arrives at the far end TJ $2a = l$ it cannot proceed growth along the same plane due to the superior strength of the grains. Consideration of the conditions under which a crack will kink onto a tilted sequent GB requires rather simple transformations of the stress intensity factors (see Cotterell and Rice 1980, Lawn and Wilshaw 1975 or Stojimirovic, et al. 1987, etc.). After some rather straightforward manipulations the maximum stress on the plane tilted at an angle of $\pi/3$ with respect to the plane of the crack is derived as

$$\sigma_{max}(\beta + \pi/3, t) = \frac{(3\sqrt{3} + \sqrt{2})K_1(\beta,t)\ -3(1 + \sqrt{2})K_2(\beta,t)}{8\sqrt{2\pi b_o}} \tag{12}$$

where K_1 and K_2 are stress intensity factors of the main crack. Thus, a crack will kink when strength (9)

$$F_k(\beta,t) = \sigma_{max}(\beta + \pi/3, t) - \sigma_{id} = 0 \qquad (13)$$

STRAINS

Once the crack opening displacements are determined as a function of time, applied stresses and material parameters they must be summed over all operative cracks within a representative element mapping on a point of an appropriately selected effective continuum.

Denote by A the surface area of a representative volume element (RVE) containing a statistically significant number N of randomly oriented grains, grain boundaries (GB) and intergranular microcracks. The RVE will be considered initially isotropic and thereafter statistically homogeneous (in the sense of an effective medium, see Kunin, 1983).

The macrostrain is then defined as in Horii and Nemat-Nasser (1983), etc. as

$$\underset{\sim}{e} = \frac{1}{A}\int_A \underset{\sim}{e}\, dA = (1 - f_c)\, \underset{\sim}{e}^e + f_c\, \underset{\sim}{e}^c \qquad (14)$$

where the three terms on the right-hand side of (14) represent the RVE average of the elastic strain and strains attributable to the GB sliding and microcracking, respectively. Also, $f_c = A_c/A$ is the the surface area density of the operative cracks. Hence, (14) can be rewritten more explicitly as

$$\underset{\sim}{e} = \frac{1}{A}\int_A \underset{\sim}{e}^e\, dA + \frac{1}{A}\sum\int_{A_c} \underset{\sim}{e}^c\, dA \qquad (15)$$

where the summation is extended over all operative defects.

The strains associated with the displacement discontinuities across the microcracks are (Horii and Nemat-Nasser 1983, Stojimirovic, et al. 1987)

$$A\, \underset{\sim}{e}^c = \int_{-a}^{a} (\underset{\sim}{b} \otimes \underset{\sim}{n})\, da \qquad (16)$$

where $\underset{\sim}{b}(\sigma,S,t)$ is the crack opening displacement (COD) of a slit with normal $\underset{\sim}{n}$ and length 2a.

The glide $\underset{\sim}{u}$ and the COD $\underset{\sim}{b}$ depend on the density and orientation of the surrounding defects as well. Within the framework of the effective media theories it will be assumed that the external fields of a particular defect weakly depend on the exact position of the adjacent defects. This assumption greatly facilitates the computations at the cost of restricting the applications to the case of low to moderate defect densities.

The details of a procedure leading to the assembly of the expressions for the strains attributable to the operative cracks can be found in Stojimirovic, et al. (1987) and Krajcinovic and Stojimirovic (t.a.) and will not be repeated here due to the constraints on the length of the paper.

ILLUSTRATIVE EXAMPLE

Using the material data from Riedel (1987) $p = 10^{-7}$ m, $\lambda = 3\ 10^{-7}$ m, $\Omega = 4.25\ 10^{-29}$ m, $\delta D_b = 8.8\ 10^{-8}$ m³/s, $D_v = 2.8\ 10^{-25}$ m²/s, one obtains $\eta = 7\ 10^{27}$ Pa s/m, $\alpha = 1.66\ 10^{-25}$ and with $E = 3.2\ 10^{11}$ N/m² (at 0.6 T), it was possible to determine all necessary parameters and perform numerical computations. For the case of tensile loading the microcrack concentrations are rather moderate allowing the use of the Taylor's model (Sumarac and Krajcinovic, 1987) at a very small loss of accuracy.

Assuming further that the grains are of uniform size (50μm) and that their orientation is the only random variable the computations turn out to be exceedingly simple. The results of these computations is presented in Fig.2.

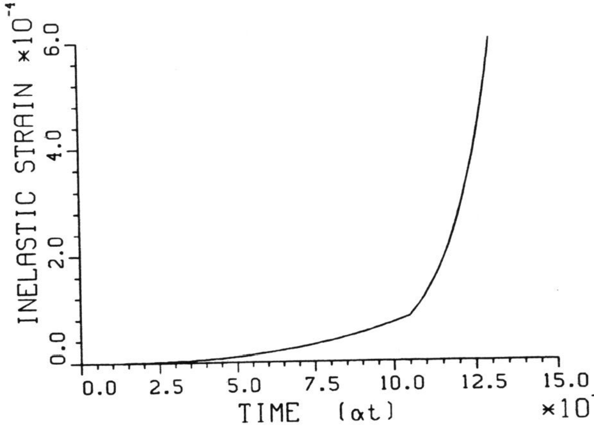

Fig.2 Macroscopic stress-strain curve for the case of uniaxial tension

The inelastic strain vs. time curve plotted in Fig.2 clearly demonstrates the effectiveness of the proposed strategy. Even more importantly it seems obvious that the salient aspects of the response may be replicated using only the physically identifiable and measurable material parameters. This, naturally, enables a rational optimization of the microstructure for a given set of circumstances.

ACKNOWLEDGEMENT

The authors gratefully acknowledge the financial support rendered by the National Science Foundation, Directorate for Engineering, Solid and Geo-Mechanics Program research grant to the University of Illinois at Chicago which made this work possible.

REFERENCES

Cotterell, B. and J.R. Rice (1980). Slightly curved or kinked cracks. *Int. J. of Fracture*, 16, 155-169.

Das, E.S.P. and M.J. Marcinkowski (1972). Accommodation of the stress field at a grain boundary under heterogeneous shear by initiation of microcracks. *J. Appl. Phys.*, 43, 4426-4434.

Evans, A.G. (1984). *Fracture in Ceramic Materials*. Noyes Publ., Park Ridge, NJ, USA.

Evans, A.G., J.R. Rice and J.P. Hirth (1980). Suppression of cavity formation in ceramics: prospects for superplasticity. *J. Amer. Ceramic Soc.*, 31, 368-375.

Frost, H.J. and F.M. Ashby (1982). Deformation-Mechanism Maps. *The Plasticity and Creep of Metals and Ceramics* Pergamon Press, London, UK.

Horii, H. and S. Nemat-Nasser (1983). Overall moduli of solids with microcracks: load-induced anisotropy. *J. Mech. Phys. Solids*, 31, 155-171.

Krajcinovic, D. and A. Stojimirovic (t.a.). Deformation processes in semibrittle polycrystalline ceramics (to appear in the Int. J. of Fracture).

Kunin, I.A. (1983). *Elastic Media with Microstructure II* Springer Verlag, Berlin.

Lau, C.W., A.S. Argon and F.A. McClintock (1983). Stress concentrations due to sliding grain boundaries in creeping alloys. In: Elastic-Plastic Fracture: Second Symposium, Vol. I (C.F. Shih and J.P. Gudas, eds.). ASTM STP 803 Publ., *Am. Soc. for Testing of Materials*, pp. I-551-572.

Lawn, B.R. and T.R. Wilshaw (1975). *Fracture of Brittle Solids* Cambridge Univ. Press, Cambridge, UK.

Raj, R. (1975). Transient behavior of diffusion-induced creep and creep rupture. *Metal. Trans. A*, 6A, 1499-1509.

Riedel, H. (1987). *Fracture at High Temperatures* Springer-Verlag, Berlin.

Stojimirovic, A., D. Krajcinovic and T. Sadowski (1987). Constitutive model for polycrystalline MgO ceramics. In: *Constitutive Modelling for Nontraditional Materials*. (Stokes, V. and D. Krajcinovic eds.), AMD-Vol. 85, ASME Publ., New York, pp. 175-188.

Sumarac, D. and D. Krajcinovic (1987). A self-consistent model for microcrack weakened solids. *Mech. of Materials*, 6, 39-52.

Tvergaard, V. (1984). Influence of the grain boundary sliding on material failure in the tertiary creep range. DCAMM Rep. No. 290. Tech. Univ. of Denmark, Lungby.

Tvergaard, V. and J.W. Hutchinson (1987). Micro-cracking in ceramics induced by thermal expansion or elastic anisotropy. MECH-96 Report, Harvard Univ., Cambridge, MA.